

Anomalous Hall effect in quaternary Heusler-type Ni₅₀Mn₁₇Fe₈Ga₂₅ melt-spun ribbons

Zhiyong Zhu, Siu Wing Or, and Guangheng Wu

Citation: *Applied Physics Letters* **95**, 032503 (2009); doi: 10.1063/1.3176479

View online: <http://dx.doi.org/10.1063/1.3176479>

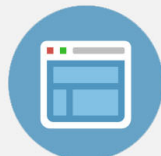
View Table of Contents: <http://scitation.aip.org/content/aip/journal/apl/95/3?ver=pdfcov>

Published by the [AIP Publishing](#)



Re-register for Table of Content Alerts

Create a profile.



Sign up today!



Anomalous Hall effect in quarternary Heusler-type $\text{Ni}_{50}\text{Mn}_{17}\text{Fe}_8\text{Ga}_{25}$ melt-spun ribbons

Zhiyong Zhu,^{1,2} Siu Wing Or,^{1,a)} and Guangheng Wu²

¹Department of Electrical Engineering, The Hong Kong Polytechnic University, Hung Hom, Kowloon, Hong Kong

²Beijing National Laboratory for Condensed Matter Physics, Institute of Physics, Chinese Academy of Sciences, Beijing 100080, People's Republic of China

(Received 17 February 2009; accepted 22 June 2009; published online 21 July 2009)

The anomalous Hall effect (AHE) in quarternary Heusler-type $\text{Ni}_{50}\text{Mn}_{17}\text{Fe}_8\text{Ga}_{25}$ melt-spun ribbons is investigated. Experimental correlation between saturated anomalous Hall resistivity (ρ_A^{MS}) and longitudinal resistivity (ρ_{xx}) is achieved for the low-temperature martensitic phase and the high-temperature austenitic phase as $\rho_A^{MS} \propto \rho_{xx}^{n=4.2}$ and $\rho_A^{MS} \propto \rho_{xx}^{n=2.1}$, respectively. The unexpectedly large exponent of $n=4.2$ in the martensitic phase is found to contradict the traditional theory of AHE with $n=1-2$, but it can be explained by a side-jump model beyond the short-range limit as a result of the intermediate-range spin-dependent electron scattering by relatively large Mn-rich clusters instead. The restoration of the exponent back to a normal value of $n=2.1$ in the austenitic phase is ascribed to the domination of the electron scattering by phonons, compared to that by the Mn-rich clusters, at elevated temperatures and with phonon softening in the transverse-acoustic TA_2 mode. © 2009 American Institute of Physics. [DOI: 10.1063/1.3176479]

Heusler alloys have attracted considerable research attention in recent years due to the discovery of the interesting ferromagnetic shape memory effect in the ternary Heusler alloy system Ni–Mn–Ga in 1996.¹ Inspired by the room-temperature ultralarge magnetic field-induced strains (MFISs) in excess of 6% in Ni–Mn–Ga single crystals, many other Heusler alloy systems have been developed, including the ternary alloy systems (Ni–Fe–Ga, Ni–Mn–Al, Co–Ni–Ga, Ni–Co–Al, etc.) and the quarternary alloy systems (Ni–Mn–Fe–Ga, Co–Ni–Ga–Fe, etc.).^{2–7} Among them, the quarternary Ni–Mn–Fe–Ga system is regarded as a valuable Heusler alloy system, featuring both MFIS and giant magnetoresistance (GMR).^{6,8} In fact, the phenomenon of GMR originates from the spin-dependent scattering of electrons by Mn-rich clusters formed under abrupt cooling,⁸ and GMR can be treated as an equal footing to anomalous Hall effect (AHE) due to the strong correlation between longitudinal resistivity (ρ_{xx}) and Hall resistivity (ρ_{xy}).⁹ However, there does not appear to be any published work reporting AHE in the quarternary Ni–Mn–Fe–Ga system even though AHE plays an important role in magnetotransport behaviors.

In ferromagnetic materials, ρ_{xy} is generally related to ordinary Hall resistivity (ρ_0) and anomalous Hall resistivity (ρ_A) by¹⁰

$$\rho_{xy}(B) = \rho_0 + \rho_A = R_0 B + R_A \mu_0 M. \quad (1)$$

In Eq. (1), ρ_0 is derived from the Lorentz force endured by charge carriers in an applied magnetic induction (B) and can be described by the product of ordinary Hall coefficient (R_0) and B . On the other hand, ρ_A is mainly caused by spin-orbit interactions between conduction electrons and disorders, such as impurities, phonons, etc., and can be expressed by the product of anomalous Hall coefficient (R_A), permeability of free space ($\mu_0 = 4\pi \times 10^{-7}$ H/m), and magnetization (M). ρ_A basically involves two distinctive mechanisms, both af-

fecting the resulting Hall effect.^{10–12} The first mechanism is “skew scattering,” which causes the electron trajectory to deflect asymmetrically from its original path. The second mechanism is “side jump,” whereby the electron trajectory is displaced transversely by a distance while the direction remains unchanged. It has been shown experimentally and theoretically that the saturated anomalous Hall resistivity (ρ_A^{MS}) has a proportional relationship to ρ_{xx} as follows:¹⁰

$$\rho_A^{MS} \propto \rho_{xx}^n, \quad (2)$$

where the exponent n is a constant and its value gives an indication of the mechanism underlying AHE. That is, if $n=1$, the skew scattering mechanism (i.e., the first mechanism) dominates AHE; if $n=2$, the side-jump mechanism (i.e., the second mechanism) controls AHE. It should be noted that n normally lies in the range of one and two for common ferromagnetic materials. For example, the well-known ferromagnetic Ni and Fe have n values of 1.5 and 2.0, respectively.¹⁰ This indicates that the skew scattering mechanism and the side-jump mechanism are both effective to AHE in Ni, while the side-jump mechanism is responsible for AHE in Fe.

In this letter, we report an unusually large n value of 4.2 (which is a surprise to most ferromagnetic materials according to the traditional AHE theory) in the low-temperature martensitic phase and a restoration of n back to a normal value of 2.1 in the high-temperature austenitic phase, both occurred in melt-spun ribbons made of a quarternary Heusler alloy $\text{Ni}_{50}\text{Mn}_{17}\text{Fe}_8\text{Ga}_{25}$. The underlying mechanism is discussed in terms of the competition between the electron scattering by phonons and that by much larger sized Mn-rich clusters.

Polycrystalline $\text{Ni}_{50}\text{Mn}_{17}\text{Fe}_8\text{Ga}_{25}$ precursor ingot was prepared by arc-melting the constituent metals in a high-purity argon atmosphere. The purities of the constituents were 99.95%. The as-prepared precursor ingot was melt-spun onto a copper wheel traveling at a linear velocity of 18 m/s in the argon atmosphere, resulting in melt-spun rib-

^{a)} Author to whom correspondence should be addressed. Electronic mail: ceswor@polyu.edu.hk.

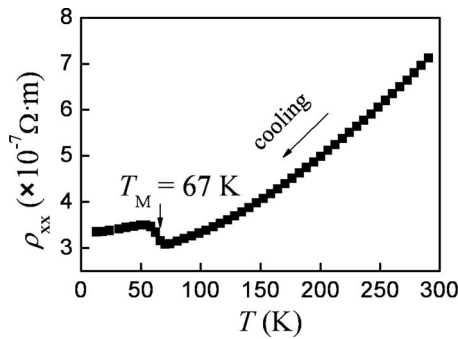


FIG. 1. Dependence of longitudinal resistivity (ρ_{xx}) on temperature (T) for $\text{Ni}_{50}\text{Mn}_{17}\text{Fe}_8\text{Ga}_{25}$ melt-spun ribbons under a typical cooling run. T_M denotes the martensitic transformation temperature.

bons of 2 mm wide and 40 μm thick. The dependence of ρ_{xx} on temperature (T) and that of ρ_{xy} on B at various T for the $\text{Ni}_{50}\text{Mn}_{17}\text{Fe}_8\text{Ga}_{25}$ melt-spun ribbons with the Hall bar configuration were measured using a Hall effect measurement system (LakeShore 7607). The M - B curves of the ribbons were evaluated at room temperature using a vibrating sample magnetometer system (LakeShore 7407). ρ_0 was deduced by linear-fitting the high- B region of the measured ρ_{xy} - B curves. ρ_A was obtained by subtracting ρ_0 from ρ_{xy} according to Eq. (1).

Figure 1 shows the dependence of ρ_{xx} on T for the $\text{Ni}_{50}\text{Mn}_{17}\text{Fe}_8\text{Ga}_{25}$ melt-spun ribbons under a typical cooling run. Martensitic transformation from the high-temperature austenitic phase to the low-temperature martensitic phase is indicated by the abrupt change in ρ_{xx} at the martensitic transformation temperature (T_M) of 67 K. It can be seen from the region around T_M that ρ_{xx} in the martensitic phase has values higher than that in the austenitic phase owing to the additional electron scattering at the twin-boundaries in the martensitic phase. The observation agrees with that for the $\text{Ni}_{50}\text{Mn}_{19}\text{Fe}_6\text{Ga}_{25}$ and Ni_2FeGa melt-spun ribbons.^{2,8}

Figure 2 illustrates the dependence of ρ_A on B at various T for the $\text{Ni}_{50}\text{Mn}_{17}\text{Fe}_8\text{Ga}_{25}$ melt-spun ribbons in the austenitic [Fig. 2(a)] and martensitic [Fig. 2(b)] phases. It is observed that the ρ_A - B curves obtained at different T show similar quantitative trends, that is, ρ_A increases monotonically with increasing B from 0 to 0.8 T and tends to level off at elevated B above 0.8 T where a relatively linear response of ρ_A to B takes place. Moreover, ρ_A decreases with decreasing T for the whole range of B , leading to higher ρ_A values in the austenitic phase [Fig. 2(a)] compared to the martensitic phase [Fig. 2(b)].

Figure 3 correlates ρ_A^{MS} with ρ_{xx} on the logarithmic scale for the $\text{Ni}_{50}\text{Mn}_{17}\text{Fe}_8\text{Ga}_{25}$ melt-spun ribbons in the austenitic [Fig. 3(a)] and martensitic [Fig. 3(b)] phases in order to in-

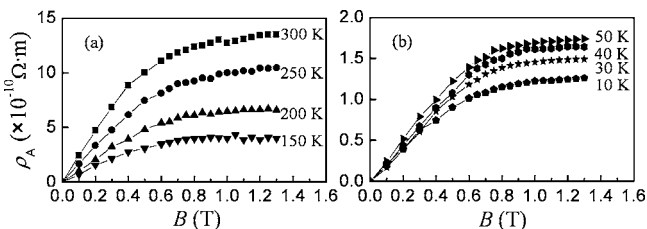


FIG. 2. Dependence of anomalous Hall resistivity (ρ_A) on magnetic induction (B) at various temperatures (T) for $\text{Ni}_{50}\text{Mn}_{17}\text{Fe}_8\text{Ga}_{25}$ melt-spun ribbons in (a) the high-temperature austenitic phase and (b) the low-temperature martensitic phase.

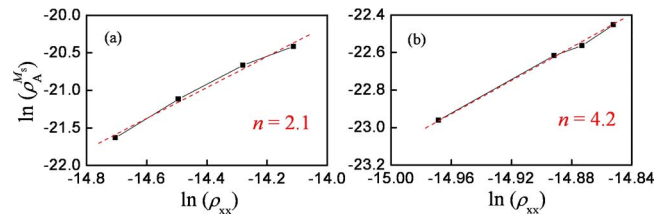


FIG. 3. (Color online) Correlation between saturated anomalous Hall resistivity (ρ_A^{MS}) and longitudinal resistivity (ρ_{xx}) on the logarithmic scale for $\text{Ni}_{50}\text{Mn}_{17}\text{Fe}_8\text{Ga}_{25}$ melt-spun ribbons in (a) the high-temperature austenitic phase and (b) the low-temperature martensitic phase. n is the slope of the $\ln(\rho_A^{MS}) - \ln(\rho_{xx})$ curve.

vestigate the underlying mechanism of AHE. It is noted that the values of ρ_A^{MS} are obtained from the measured ρ_A - B curves (Fig. 2) by extracting ρ_A value at $B=1.3$ T for each temperature (T), while the values of ρ_{xx} are acquired from the measured ρ_{xx} - T plot (Fig. 1) at the corresponding T of ρ_A^{MS} . Using the proportional relationship $\rho_A^{MS} \propto \rho_{xx}^n$ described in Eq. (2),¹⁰ the value of the exponent n in ρ_{xx} is evaluated for each of the two phases by determining the slope of the respective $\ln(\rho_A^{MS}) - \ln(\rho_{xx})$ plot in Fig. 3. For the high-temperature austenitic phase in Fig. 3(a), $n=2.1$ is obtained, suggesting that the side-jump mechanism has the predominant effect in this phase and the theoretical correlation $\rho_A^{MS} \propto \rho_{xx}^2$ is valid. For the low-temperature martensitic phase in Fig. 3(b), although ρ_{xx} shows a very limited range of variation, an extraordinary large n of 4.2, contradicting the traditional theory of AHE with $n=1-2$, is acquired instead.

The authors believe that the extraordinary large n of 4.2 observed in the low-temperature martensitic phase in Fig. 3(b) can be explained by a special side-jump model, namely, the side-jump model beyond the short-range limit.⁹ In this special side-jump model, the short-range assumption adopted in the traditional side-jump model involving small fluctuations in scattering potential (such as phonon excitations and dilute impurities) caused by scatters with sizes much smaller than the atomic dimensions is released and extended to the intermediate range so that the following expression holds true:

$$\rho_A^{MS} \propto \rho_{xx}^{2+\alpha}, \quad (3)$$

where the exponent α is a constant relating to the transverse side jump per collision influenced by the scattering potential. It is noted that if α in Eq. (3) vanishes, the traditional side-jump mechanism with $n=2$ is restored. Thus, the extraordinary large n value of 4.2 in our ribbons can be accounted for $\alpha=2.2$ according to the special side-jump model presented in Eq. (3). The reason why this special side-jump model can be adopted in our ribbons is clarified as follows. Actually, an extraordinary large n value of 3.7, corresponding to $\alpha=1.7$, has also been reported in Co-Ag granular structures comprising Co particles (acting as the scatters) of a few nanometers—a breakdown of the short-range assumption.⁹ Here, it turns to an important question about the minimal sizes of the scatters required to make the traditional side-jump model invalid in our ribbons. As GMR in the Ni-Mn-Fe-Ga melt-spun ribbons is known to originate from the spin-dependent scattering of electrons by Mn-rich clusters formed under abrupt cooling,⁸ one of the necessary conditions for enabling the GMR phenomenon is to ensure the sizes of the scatters on a microscopic length scale of the mean free path of about few nanometers.¹³ Due to the fact

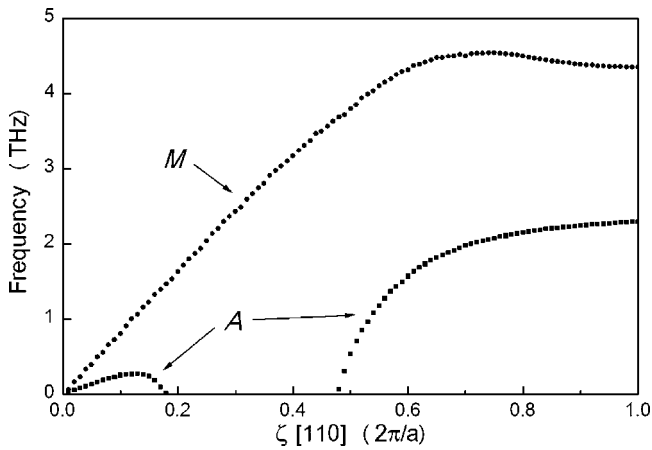


FIG. 4. Transverse-acoustic TA_2 mode of the photon spectrum of the cubic austenitic (A) phase and the tetragonal martensitic (M) phase for Ni_2MnGa . The data are obtained from Fig. 2 of Ref. 15, where the photon spectrum has been computed using the first-principles method based on density functional theory. The reduced wave vector coordinate ζ , which is the same as that in Ref. 15, spans the fcc Brillouin zone from Γ to X.

that GMR has been manifested in both our Ni–Mn–Fe–Ga melt-spun ribbons and the Co–Ag granular structures, the size scale of the Mn-rich clusters presented in our Ni–Mn–Fe–Ga melt-spun ribbons should have the same order of magnitude as the Co particles in the Co–Ag granular structures. Therefore, it is reasonable to infer that when the spin-dependent electron scattering by the Mn-rich clusters are dominant, the short-range assumption should also break down in our ribbons and the special side-jump model should be adopted.

Another issue concerned in the AHE in our $Ni_{50}Mn_{17}Fe_8Ga_{25}$ melt-spun ribbons is the restoration of the exponent n from a large value of 4.2 in the low-temperature martensitic phase back to a normal value of 2.1 in the high-temperature austenitic phase. The authors also found that this restoration of n can be understood by the competition between the electron scattering by phonons and that by the relatively large Mn-rich clusters. On the one hand the electron scattering by the Mn-rich clusters (which can be viewed as a kind of impurity) is independent of temperature, and on the other hand both the experimental and theoretical investigations on the phonon-dispersion relations of Ni_2MnGa (the base material of our $Ni_{50}Mn_{17}Fe_8Ga_{25}$ melt-spun ribbons) reveal the occurrence of phonon softening beyond the martensitic transformation temperature.^{14,15} As part of the photon spectrum, the transverse-acoustic TA_2 mode of the cubic austenitic (A) phase and the tetragonal martensitic (M) phase for Ni_2MnGa is shown in Fig. 4.¹⁵ The data are obtained from Fig. 2 of Ref. 15 where the photon spectrum has been computed using the first-principles method based on density functional theory. The reduced wave vector coordinate ζ , which is the same as that in Ref. 15, spans the fcc Brillouin zone from Γ to X. From Fig. 4, it is clear that phonon softening in the A phase leads to an increase in the number of the low-frequency vibration modes with respect to the M phase. Based on the thermodynamics of crystal lattice, the number of phonons of a certain vibration mode $n(\omega_i)$ declines exponentially with $\hbar\omega_i/k_B T$ (where \hbar is the reduced Planck constant, ω_i is the mode frequency, k_B is the Boltzmann constant, and T is the temperature) as follows:¹⁶

$$n(\omega_i) = \frac{1}{e^{\hbar\omega_i/k_B T} - 1}. \quad (4)$$

It can be seen that low-frequency vibration modes give the greatest contribution to the electron-phonon scattering in the low-temperature region.¹⁶ Therefore, the electron scattering by phonons should be much stronger in the high-temperature austenitic phase than in the low-temperature martensitic phase. Accordingly, it is reasonable to believe that the electron scattering by phonons plays the predominant role in the austenitic phase compared to the electron scattering by the Mn-rich clusters in our $Ni_{50}Mn_{17}Fe_8Ga_{25}$ melt-spun ribbons, leading to a restoration of n from a large value of 4.2 back to a normal value of 2.1 (conforming to the traditional AHE theory).

In summary, we have prepared quaternary Heusler-type $Ni_{50}Mn_{17}Fe_8Ga_{25}$ melt-spun ribbons and investigated their AHE. According to the relationship $\rho_A^{M_{50}} \rho_{xx}^n$, an unusually large n of 4.2, which contradicts the values of one to two in the traditional theory of AHE, has been determined experimentally for the low-temperature martensitic phase and explained using a side-jump model beyond the short-range limit as a result of the predominant intermediate-range spin-dependent electron scattering by large Mn-rich clusters. On the other hand, a normal n value of 2.1, conforming to the traditional AHE theory, has been observed for the high-temperature austenitic phase. The restoration of n value from 4.2 (in the martensitic phase) to 2.1 (in the austenitic phase) has been attributed to the elevation in temperature and the phonon softening in TA_2 mode whereby the electron scattering by phonons becomes dominant and prevails over that by the Mn-rich clusters.

This work was supported by the Research Grants Council of the HKSAR Government (Grant No. PolyU 5257/06E) and the Central Research Grant of The Hong Kong Polytechnic University (Grant No. A-PA3C).

¹K. Ullakko, J. K. Huang, C. Kantner, R. C. O'Handley, and V. V. Kokorin, *Appl. Phys. Lett.* **69**, 1966 (1996).

²Z. H. Liu, M. Zhang, Y. T. Cui, Y. Q. Zhou, W. H. Wang, G. H. Wu, X. X. Zhang, and G. Xiao, *Appl. Phys. Lett.* **82**, 424 (2003).

³A. Fujita, K. Fukamichi, F. Gejima, R. Kainuma, and K. Ishida, *Appl. Phys. Lett.* **77**, 3054 (2000).

⁴M. Wuttig, J. Li, and C. Craciunescu, *Scr. Mater.* **44**, 2393 (2001).

⁵K. Oikawa, L. Wulff, T. Iijima, F. Gejima, T. Ohmori, A. Fujita, K. Fukamichi, R. Kainuma, and K. Ishida, *Appl. Phys. Lett.* **79**, 3290 (2001).

⁶Z. H. Liu, M. Zhang, W. Q. Wang, W. H. Wang, J. L. Chen, G. H. Wu, F. B. Meng, H. Y. Liu, B. D. Liu, J. P. Qu, and Y. X. Li, *J. Appl. Phys.* **92**, 5006 (2002).

⁷X. F. Dai, G. D. Liu, Z. H. Liu, G. H. Wu, J. L. Chen, F. B. Meng, H. Y. Liu, L. Q. Yan, J. P. Qu, Y. X. Li, W. G. Wang, and J. Q. Xiao, *Appl. Phys. Lett.* **87**, 112504 (2005).

⁸Z. H. Liu, H. Liu, X. X. Zhang, X. K. Zhang, J. Q. Xiao, Z. Y. Zhu, X. F. Dai, G. D. Liu, J. L. Chen, and G. H. Wu, *Appl. Phys. Lett.* **86**, 182507 (2005).

⁹P. Xiong, G. Xiao, J. Q. Wang, J. Q. Xiao, J. S. Jiang, and C. L. Chien, *Phys. Rev. Lett.* **69**, 3220 (1992).

¹⁰L. Berger and G. Bergmann, in *The Hall Effect and Its Applications*, edited by C. L. Chien and C. R. Westgate (Plenum, New York, 1979), p. 55.

¹¹J. Smit, *Physica (Utrecht)* **21**, 877 (1955); **24**, 39 (1958).

¹²L. Berger, *Phys. Rev. B* **2**, 4559 (1970).

¹³J. Q. Xiao, J. S. Jiang, and C. L. Chien, *Phys. Rev. Lett.* **68**, 3749 (1992).

¹⁴A. Zheludev, S. M. Shapiro, P. Wochner, and L. E. Tanner, *Phys. Rev. B* **54**, 15045 (1996).

¹⁵A. T. Zayak, P. Entel, J. Enkovaara, A. Ayuela, and R. M. Nieminen, *Phys. Rev. B* **68**, 132402 (2003).

¹⁶J. M. Ziman, *Electrons and Phonons* (Oxford University Press, London, 1960).